GPS Multipath and Its Relation to Near-Surface Soil Moisture Content

Kristine M. Larson, John J. Braun, Eric E. Small, Valery U. Zavorotny, *Senior Member, IEEE*, Ethan D. Gutmann, and Andria L. Bilich

***Abstract*—Measurements of soil moisture at various spatial and temporal scales are needed to study the water and carbon cycles. While satellite missions have been planned to measure soil moisture at global scales, these missions also need ground-based soil moisture data to validate their observations and retrieval algorithms. Here, we demonstrate that signals routinely recorded by Global Positioning System (GPS) receivers installed to measure crustal deformation for geophysical studies could be used to provide a global network of soil moisture sensors. The sensitivity to soil moisture is seen in reflected GPS signals, which are quantified by using the GPS signal to noise ratio data. We show that these data are sensitive to soil moisture variations for areas of 1000 m2 horizontally and 1–6 cm vertically. It is demonstrated that GPS signals penetrate deeper when the soil is dry than when it is wet. This change in penetration or "reflector" depth, along with the change in dielectric constant, causes the GPS signal strength to change its frequency and amplitude. Comparisons with conventional water content reflectometer sensors show good agreement ($r^2 = 0.9$ to 0.76) with the variation in frequencies of the reflected GPS signals over a period of 7 months, with most of the disagreement occurring when soil moisture content is less than 0.1 cm^3/cm^3.**

***Index Terms*—Global positioning system, remote sensing, soil measurements.**

I. Introduction

SOIL moisture is a key component of the water cycle budget. Soil moisture influences the sensible and latent heat flux from the land surface to the atmosphere. At large scales, these fluxes affect weather patterns [1], [2], and locally, the availability of moisture at the surface is of critical importance for plant growth [3], [4]. As such, assessing the long-term changes in soil moisture is important for the carbon cycle and agriculture. Soil moisture also influences drought and flooding [5], [6] and plays an important role in climate change [2], [7].

To monitor soil moisture globally, both the National Aeronautics and Space Administration (NASA) and the European Space Agency (ESA) have proposed satellite missions. The NASA Soil Moisture Active Passive (SMAP) mission is expected to be launched sometime after 2013. This satellite will provide surface soil moisture estimates with a pixel size around 10 km by employing a combination of L-band active and passive microwave sensors [8]. The ESA Soil Moisture and Ocean Salinity (SMOS) mission is scheduled for launch in 2010. SMOS will yield estimates of surface soil moisture with a pixel size around 50 km derived from a L-band passive microwave sensor [9], [10]. Combined with assimilation models, data from these satellites will provide unprecedented spatial coverage of the soil state, but they must first be validated with ground-based soil moisture observations.

Ground-based or *in situ* measurements are made at many locations around the world, but their utility for regional and continental studies is restricted for a variety of reasons. For example, availability of these datasets is often limited and combining data from different types of *in situ* sensors is difficult. And since soil moisture is spatially variable, measurements made over small volumes (~1 liter), such as used by SCAN (Soil Climate Analysis Network), will not be representative of a region. Ideally *in situ* networks should sense large spatial regions (hundreds of meters) and provide information about both soil moisture at the surface and throughout the root zone. Recently, [11] demonstrated that cosmic-ray neutrons could be used to provide soil moisture estimates over large spatial-scales (~300 m radius) averaged over a depth of several decimeters. In this paper, we describe how continuously-operating GPS receivers could be used to estimate soil moisture variations over similar spatial scales (~50-m radius). In contrast to the cosmic-ray method, the GPS-derived signal is influenced most strongly by near-surface (0–5 cm) soil moisture, similar to the SMOS and SMAP datasets.

GPS remote sensing was first proposed 15 years ago [12]. [13] provides a demonstration of GPS remote sensing as applied to soil moisture. In GPS remote sensing, the investigators traditionally propose that the GPS receiver/antenna system be flown on an aircraft/satellite with the GPS antenna facing the ground. The receiver must be specially designed to measure reflected signals. The idea that traditional ground-based GPS receivers (where the antenna is facing up) could be used to sense soil moisture was first discussed by [14]. In that paper it was

Manuscript received February 28, 2009; revised July 31, 2009. First published November 10, 2009; current version published February 24, 2010. This work was supported in part by a University of Colorado Seed Grant, NSF ATM 0740515 (CU), and NSF ATM 0740498 (UCAR). NCAR is supported by the National Science Foundation.

K. M. Larson is with the Department of Aerospace Engineering Sciences, University of Colorado, Boulder, CO 80309 USA (e-mail: kristinem.larson@gmail.com).

J. J. Braun is with COSMIC, University Corporation for Atmospheric Research, Boulder, CO 80301 USA (e-mail: braunj@ucar.edu).

E. E. Small is with the Department of Geological Sciences, University of Colorado, Boulder, CO 80309 USA (e-mail: eric.small@colorado.edu).

V. U. Zavorotny is with the Earth Systems Research Laboratory, National Oceanic and Atmospheric Administration, Boulder, CO 80305 USA (e-mail: valery.zavorotny@noaa.gov).

E. D. Gutmann is with Research Applications Laboratory, National Corporation for Atmospheric Research, Boulder, CO 80307 USA (e-mail: gutmann@ucar.edu).

A. L. Bilich is with the National Geodetic Survey at the National Oceanic and Atmospheric Administration, Boulder, CO 80305 USA (e-mail: andria.bilich@noaa.gov).

Color versions of one or more of the figures in this paper are available online at http://ieeexplore.ieee.org.

Digital Object Identifier 10.1109/JSTARS.2009.2033612

noted that changes in GPS signal strength correlated with precipitation and the expected dry-downs at a continuously-operating GPS site in Uzbekistan. However, that study was limited by the lack of *in situ* soil moisture instruments at the GPS site. A subsequent study conducted at Marshall, CO, summarized data from a GPS system and ten water content reflectometers buried at depths of 2.5 and 7.5 cm [15]. Modeled GPS signal strength data showed a correlation of 0.91 with the shallow water content reflectometers over a period of 83 days. In this study, we extend the Marshall experiment to span 210 days, providing a more robust comparison between the water content reflectometers and the GPS method. We have further expanded our analysis to include an assessment of reflector depth and how it varies through time. We also compared records from an identical receiver and antenna with and without a radome. A companion paper provides the theoretical basis for these results [16].

Because they use existing infrastructure, continuously-operating GPS systems could provide a cost-effective method of calibrating large-scale (>1 km) soil moisture measurements for three reasons. First, there are over 2000 continuously-operating GPS systems in the U.S. alone. They are located on and near a wide range of soil and vegetation types. Second, GPS instruments are sensitive to a larger area of the ground ($\sim 1000\ \mathrm{m}^2$) [15] than traditional soil moisture instruments (tens of centimeters) [17]. Third, the GPS signal is L-band, and, therefore, its sensitivity to soil moisture and vegetation is similar to those from both SMAP and SMOS.

II. Characteristics of a Geodetic-Quality Continuously-Operating GPS Site

In this study we focus on data that could potentially be provided by existing, permanent, continuously-operating "geodetic-quality" GPS sites (Fig. 1). A map of the stations whose data are freely available within 24 h of collection is shown in Fig. 2. These stations represent a heterogeneous network that has been installed and is operated by local surveyors, state and local government agencies, and the federal government. In the western U.S., many of the stations are part of the EarthScope Plate Boundary Observatory (PBO), a network of 1100 GPS stations installed and operated by the National Science Foundation (NSF). In the eastern parts of the U.S., most of the sites are part of the Continuously-Operating Reference Station (CORS) network managed by the National Geodetic Survey (NGS). Unlike PBO, the NGS did not install and does not maintain the vast majority of the sites represented in their database; rather, they archive and distribute all CORS data, and provide positioning services for CORS. The variety of partners makes the NGS CORS network instrumentation and installation characteristics much more heterogeneous than the PBO network.

Our discussion draws examples from PBO stations due to the well-characterized nature of this network's equipment and site locations. In general, there are three specific components of a geodetic GPS site that make them suitable for soil moisture sensing: the receiver, the antenna, and how and where the antenna is attached to the ground (we will call the latter "monumentation.") The first, and most significant, component of these sites is the GPS receiver. These instruments track signals

Fig. 1. Continuously operating geodetic quality GPS receiver operating as part of the Earthscope Plate Boundary Observatory. This site in Marshall, CO, was used for the GPS soil moisture calibration study.

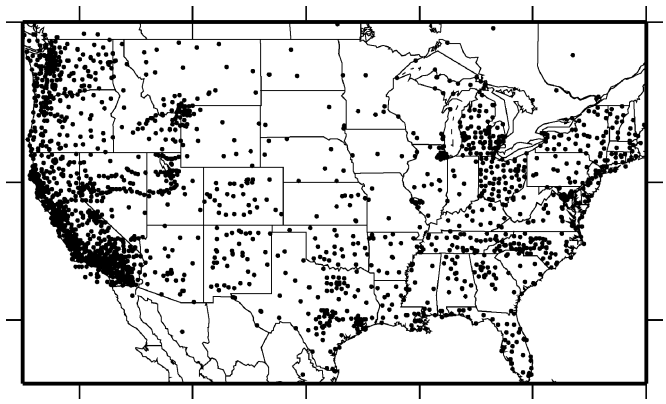

Fig. 2. Locations of geodetic-quality continuously operating GPS sites with data that are free and publicly available. Most of the sites in the western U.S. are associated with the Plate Boundary Observatory (http://www.earthscope.org). Sites in the east are coordinated by the National Geodetic Survey (http://www.ngs.noaa.gov/CORS).

generated on both GPS frequencies ($\mathrm{L1} = 1.57542$ GHz and $\mathrm{L2} = 1.22760$ GHz) and produce carrier phase and pseudorange observables. Geodesists use the highly precise (1–2 mm noise level) carrier phase observations to compute station positions that are accurate to a few millimeters in 3-D space. Observations from both frequencies are processed together using a linear combination of the observations that eliminates the range errors associated with the propagation of these signals through the ionosphere. Dual-frequency carrier-phase capabilities make a geodetic-quality receiver an order of magnitude more expensive than the L1 pseudorange instruments that are commonly used for meter-level positioning applications.

The second component of these sites is the GPS antenna. Geodetic antennas are optimized to provide tracking capabilities at all elevation and azimuth angles above the horizon. Most geophysicists in the U.S. (and all of the PBO sites) use the choke-ring GPS antenna (see Fig. 3), which is machined out of aluminum. The electrical phase center is located at the center of the choke-ring. The rings in the antenna are one quarter of the L1-wavelength (~19 cm) deep, which creates a high-impedance surface, thus reducing multipath. This antenna

Fig. 3. Top view of the antenna used by the Plate Boundary Observatory and many other geodetic-quality GPS receivers.

has a nearly azimuthally symmetric gain and phase center pattern, which is helpful for geodetic applications. Unfortunately, some of that azimuthal symmetry is sacrificed when a radome is placed over the antenna to protect it from decay due to the elements. PBO uses a radome at all its sites; it is made of a polyester and polycarbonate plastic [18]. The radomes are shaped into a hemispherical form using an injection molding procedure so that the dome is uniform in thickness and shape. Tests indicate that the walls of the dome are approximately uniform (better than 0.1 mm) in azimuth. While great care was taken in the manufacturing of these radomes, they do slightly alter both the gain pattern and mean electrical phase center of the antenna.

The final component of these sites is the monumentation of the GPS equipment. The network of geodetic-quality GPS sites shown in Fig. 2 vary in their quality for use in observing soil moisture. In the western U.S., geophysicists use geodetic-quality GPS receivers/antennas to measure tectonic motions. To ensure that the observed motions are related to the deformation of the Earth's crust, geophysicists make special efforts to tie the GPS antenna to bedrock. For example, the PBO sites (Figs. 1 and 2) have constructed their "monuments" by drilling tens of meters through soil, sediments or rocks to create a tripod-like structure that is firmly fixed to the ground. All but a handful of the PBO antennas have been installed $\sim$1.8 m above the ground. In addition, the PBO sites in the western U.S. are typically located in rural areas with few buildings. Many of these sites are suitable for use as soil moisture sensors. In contrast, stations in the eastern U.S. are frequently located on buildings and in urban environments, making them less suitable for soil moisture applications. While it is unclear at this time how many of these existing GPS stations might be immediately useful for soil moisture applications, even a fraction of these sites would provide a distributed network that is not available with current observational systems.

III. Characteristics of Geodetic-Quality GPS SNR Data

The primary data produced by geodetic-quality GPS receivers are carrier-phase and pseudorange observables [19]. A third type of observation is also generated from these instruments: the signal-to-noise ratio (SNR). Prior to its application to measure soil moisture [14], the SNR observable was used primarily as a diagnostic engineering measurement to assess signal quality and local electromagnetic noise characteristics. An SNR measurement is simply the ratio of the signal power to the measurement noise. It is frequently expressed using a logarithmic decibel (dB) or decibel-Hertz (dB-Hz) scale.

One of the most important sources of error in GPS observations is multipath. Multipath signals reflect off the ground before arriving at the GPS antenna; they create constructive and destructive interference patterns that cause oscillations in the GPS observations. The frequency of the oscillations is dependent on the GPS frequency and the distance of the reflecting surface from the antenna. Changes in the dielectric properties of the reflecting surface (e.g., changes in soil moisture) also induce changes in these periodic oscillations. The geometric relationships driving multipath oscillations in pseudorange, carrier phase, and SNR data are not derived here, but can be found in [20]. Although multipath oscillations are present in all GPS observables, it can be difficult to quantify them. The most precise GPS observation is the carrier phase, but these data require significant data processing to model orbits, clocks, and atmospheric delays before the multipath signature can be assessed. Furthermore, since carrier phase data from many satellites are analyzed simultaneously with least squares adjustment, multipath effects from one satellite will be spread into residuals for other satellites [21]. This means that one cannot as easily determine which particular soil region is responsible for multipath effects in least squares residuals. In this study, SNR data are used because GPS receiver tracking loops estimate SNR data independently for individual satellites. In this way, the source of the multipath can be readily assigned to a particular satellite and sensing area on the ground.

SNR observations are a function of the strength of the incoming signal, the gain pattern of the antenna, and the tracking algorithms used within the receiver. The GPS satellites are designed to illuminate the Earth's surface with a signal of nearly uniform power. In practice, the signal from a GPS satellite that is located at a low elevation angle will have slightly lower strength than a satellite at zenith. This variation affects direct signal strength and does not have a significant impact on the results presented here. [16] discusses the antenna gain pattern and how it affects SNR data from a theoretical perspective. These theoretical descriptions provide an important basis in the understanding of how the SNR data generated by a receiver are related to signals reflecting from a planar surface. Unfortunately this theoretical knowledge does not completely describe how a GPS receiver determines SNR in practice. This leads to the final factor that impacts SNR observations: the internal tracking algorithms used within the receiver. These algorithms can have a significant influence on the quality and precision of SNR data [22] and, thus, their usefulness for soil moisture applications. These tracking algorithms are also proprietary for each receiver manufacturer, making it difficult to understand their differences in much detail.

The GPS constellation is in the process of modernizing, which will yield new signals appropriate for soil moisture sensing. The original operational Block II constellation (designated the Block II, IIA, IIR segments) used two codes, the C/A

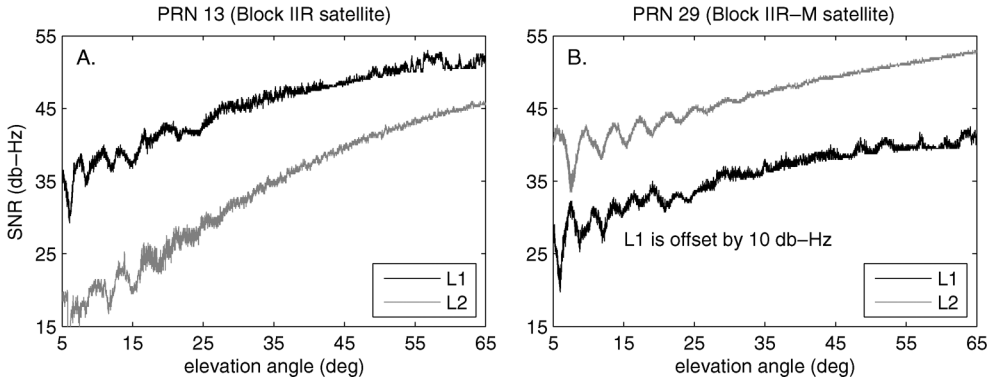

Fig. 4. a) L1 and L2 SNR data for PRN 13, a Block IIR satellite; b) L1 and L2 SNR data for PRN 29, a Block IIR-M satellite. The L1 SNR data have been offset by 10 dB-Hz for clarity.

(coarse or civilian/access) and the P (precise) codes. The P-code is used on both L1 and L2, but the C/A code was originally only on L1. As their names imply, the P-code is much more precise than the C/A code. But more importantly, the P-code has been encrypted since 1994. Only military users have full access to the P-code. In response to strong civilian interest in a civilian code on L2, satellites launched beginning in September 2006 now have a code called L2C. These are known as Block IIR-M satellites. At this writing there are six Block IIR-M satellites: satellites 7, 12, 15, 17, 29, and 31. These numbers correspond to their pseudorandom noise (PRN) codes. (For more detailed descriptions of the different Blocks of GPS satellites, see [19].)

The data presented in this paper were collected using the Trimble NetRS receiver. This receiver is a standard positioning system instrument that is marketed for the civilian community, and, thus, it does not have access to the encrypted P-code. It tracks the un-encrypted C/A code on the L1 carrier frequency. On the L2 carrier, it uses a proprietary tracking method which produces a P-code-like observable (known as P2) for older Block II satellites. Because it does not use the actual P-code for the correlation process, the SNR is much lower power than it would be for true P2. For the newer Block IIR-M satellites, the receiver is able to track the un-encrypted L2C code, producing observations with significantly higher SNR strength than the tracking methods used for encrypted data.

Representative SNR observations from an older Block IIR satellite and a new Block IIR-M satellite are shown in Fig. 4. These two figures provide clear examples of the differences in how this particular type of receiver tracks SNR observations. First, the difference in tracking power between the L1 and L2 signals in the older GPS satellites can clearly be noticed in Fig. 4(a). This 20 dB-Hz difference is related to the strength of the signal tracked using the C/A code correlator as compared to the correlator tracking the encrypted L2 carrier frequency. In Fig. 4(b) we compare L1 and L2 SNR data from a Block IIR-M satellite where both observables were derived from tracking where the code is not encrypted. In principle, one might think the data of the two SNRs should be equivalent, but they clearly are not. The L1 SNR data are much less precise than the L2 SNR. This is related to the new L2C code being more robust than the L1 C/A code.

The periodic pattern created by the multipath signal is easily seen in the L2C-SNR observations at lower elevation angles (5–25 degrees). For this reason, as with [15], we have exclusively focused on observations from the Block IIR-M satellites, whose behavior closely resembles our theoretical understanding of how multipath signals influence SNR observations. We also provide examples of L2C SNR data where a second-order polynomial has been removed (Fig. 5). While there are some differences between satellites and antennas, these variations are small compared with the oscillations resulting from ground reflections. These are the signals we are interested in for measuring soil moisture.

IV. Experimental Setup—Marshall Field

The National Center for Atmospheric Research (NCAR) observational facility in Marshall, CO, was used for this experiment. The soil in this area is classified as a cobbly clay loam. The soil in the top 5 to 10 cm of the profile is coarser than expected for a clay loam, with the sand fraction exceeding 80%. Vegetation at the site is sparse and is classified as short-grass steppe (Fig. 1). The surface is nearly horizontal, sloping $\sim$1% down to the east. Animal burrowing is the primary source of surface roughness on the otherwise planar surface, yielding broad mounds less than 10 cm in height. The Marshall site was chosen for its convenient access, good sky visibility, redundant meteorological observations, and the presence of an existing PBO GPS station. Two temporary GPS stations were installed within 50 m of the PBO station, using Trimble NetRS receivers and choke-ring antennas. To assess the impact of the protective radomes, a standard SCIGN radome was placed over one of the antennas while the second antenna was left uncovered.

The approximately 1.8 m antenna height used at Marshall allows sensing of an ellipse with maximum dimensions of $\sim$4 by 50 m (Fig. 6). The sensed area is described using the first Fresnel zone, which is defined by the semi-major axis (a) and semi-minor axis (b) of an ellipse

$$a = \frac{\sqrt{\lambda h \sin E}}{(\sin E)^2}; \quad b = \frac{\sqrt{\lambda h \sin E}}{\sin E} \tag{1}$$

where h is the height above the horizontal reflector, λ is the GPS wavelength and E is the elevation angle of the satellite

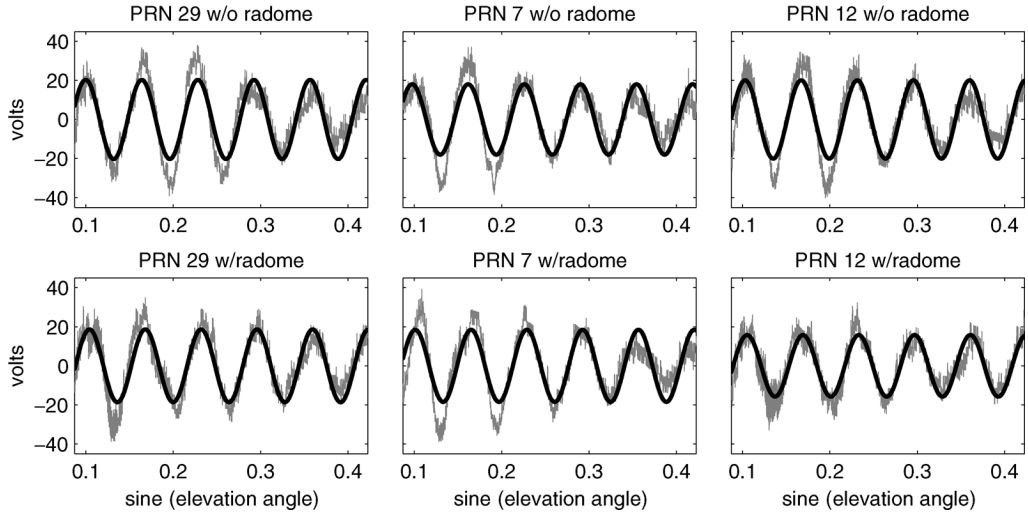

Fig. 5. L2 SNR data (gray) for three Block IIR-M satellites (29, 7, and 12). Left: Data for a choke-ring antenna with a radome; right: data from a choke-ring antenna. A constant frequency sinusoid fit (black) is also shown for each satellite.

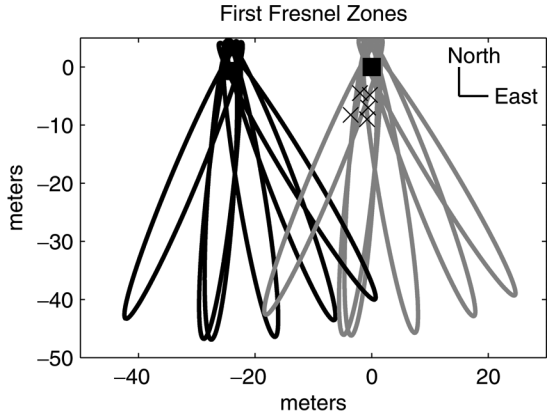

Fig. 6. First Fresnel zones at the Marshall test site for the 6 Block IIR-M GPS satellites plotted for an elevation angle of 5 degrees. As the satellites elevation angles increase, the Fresnel zones become smaller and are closer to the antenna (shown as black squares). Only the southern satellite tracks are shown. Black fresnel zones are for the choke-ring antenna and the gray fresnel zones are for the choke-ring antenna with radome. Locations of water content reflectometers are shown as crosses.

[23]. The ellipse is located along the satellite ground track, with the long axis paralleling the satellite-antenna vector. The ellipse becomes smaller and moves closer to the antennas as a satellite rises. A GPS satellite takes about an hour to rise from an elevation angle of 5 to 25 degrees.

V. Data Analysis

The observations from each satellite are analyzed independently, with each track separated into ascending and descending paths. The SNR data are converted from dB-Hz units to volts; then, a second-order polynomial is removed. As noted previously [14], multipath reflections above a horizontal planar reflector will have a frequency of

$$f = \frac{4\pi h}{\lambda} \cos E \frac{dE}{dt}. \tag{2}$$

By using sine of the elevation angle $(\sin E)$ as the independent variable, the oscillation frequency becomes a constant function of h. This multipath frequency modulates the SNR as

$$\mathrm{SNR} = A \cos\left(\frac{4\pi h}{\lambda} \sin E + \phi\right). \tag{3}$$

An unweighted least squares fit to the GPS SNR data (restricted to 5–25 degrees elevation angles) was used to find amplitude A and phase offset ϕ.

In [15], we showed by simulation that ϕ directly relates to the apparent reflection depth of the GPS signal. When the soil is wet, the apparent reflector is close to the surface; as it dries, the reflection depth is several cm deeper. As confirmed by [16], the effects of soil moisture variations are also evident in the SNR amplitude A, but will not be discussed in this paper. We have extended our analysis to independently solve for the height of the multipath reflector (h) using a Lomb–Scargle periodogram method [24]. This analysis technique provides a way to compute the spectral power at specified frequencies for an irregularly spaced time series. For each satellite trace, the frequency (f) of peak power is first identified and then translated into a reflector height, which is the vertical distance between the electrical phase center of the antenna and the apparent ground reflection planar surface. The computation of this reflector height allows for additional understanding of how deeply the reflected signals are penetrating the soil. Currently, the reflector depths are estimated with a precision of 3 mm.

Since the reflector height is defined with respect to a poorly known electrical phase center, we conducted a separate experiment to confirm the height of the antenna's electrical phase center above the ground surface. We temporarily installed a wire mesh with a width of 4 m and length of 31 m along the azimuthal ground track of PRN 31, covering the first Fresnel zone so that reflections could not penetrate into the subsurface. Reflector height was estimated for two days before and after the metal was in place. We found that the effective reflector depth is 5 ± 1 cm below the ground surface when the soil is relatively

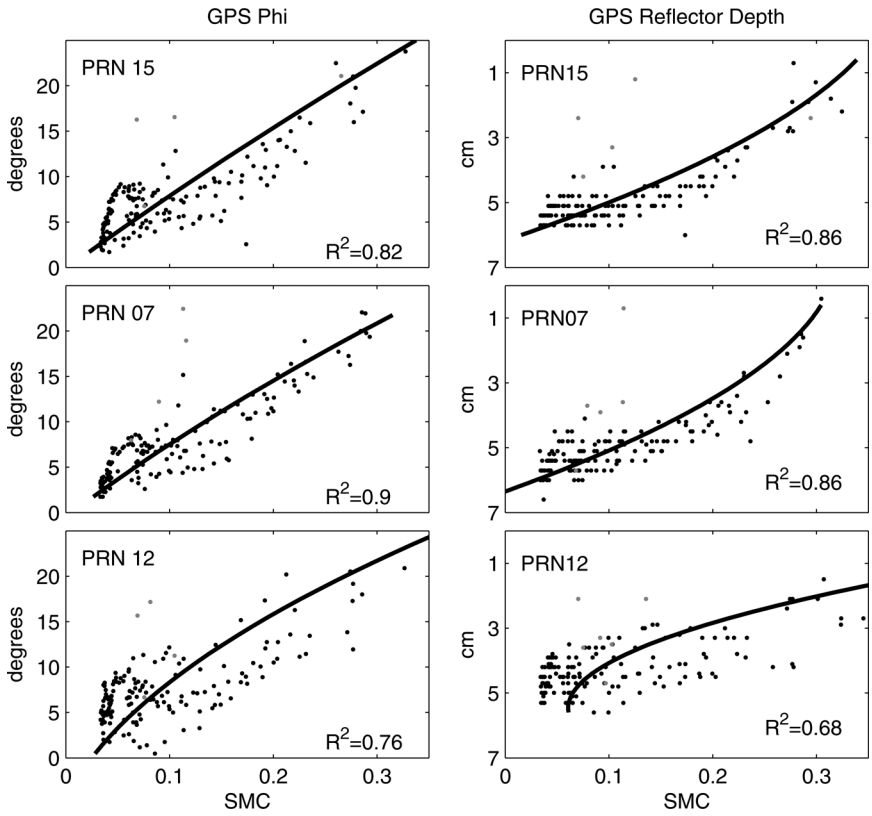

Fig. 7. Comparison of soil moisture content (SMC) measured at 2.5 cm (average of five sensors) and estimated ϕ (left column) and h (right column) for satellites 15, 7, and 12. The antenna with a radome was used in this example. Values in grey are for rainy days 157, 220, 280, and 286. See text for further discussion. h is resolved with a precision of 3 mm.

dry (0.1 soil moisture content at 2.5-cm depth). Variations in effective reflector depth are discussed below.

Variability between the SNR data from the six Block IIR-M satellites (Fig. 5) is introduced by several spatial factors, including the antenna gain pattern and properties of the ground sensed. Geometric relationships show that if the antenna gain pattern was azimuthally symmetric and the Marshall surface was truly horizontal, the SNR variations caused by multipath would be the same for all satellites. Because we do not have calibrations for the gains, some of the observed variations between SNR data are due to the antenna. Similarly, the SNR data will vary because the two antennas ($\sim$24 m apart) sense different soil surfaces, which are neither planar nor horizontal (Fig. 6).

To compare estimated ϕ and h with measured Soil Moisture Content (SMC), Campbell Scientific water content reflectometers (WCR) were installed at various depths at the Marshall site. These probes measure the time for the reflection of an electric pulse sent down two wave guides in the soil, which is related to the dielectric constant of the soil [25]. The relationship between reflection time period and SMC was calibrated gravimetrically in the lab using soil from the site. The calibration is accurate to 1% moisture content, and was consistent with 24 field samples collected on 3 separate days. Five probes were installed at 2.5 cm and five at 7.5 cm depth, to measure SMC in the 0–5 cm and 5–10 cm depth range [17]. SMC measurements were made every 15 min.

These *in situ* observations only provide estimates of soil moisture for two depth ranges, approximately 0–5 cm and 5–10 cm. The soil moisture estimates derived from the SNR data are representative of a variable depth. To facilitate the comparison of these two different measures of near-surface soil moisture, we use a standard 1-D model of water flow through variably saturated soil [26]. We selected soil hydraulic properties that yielded reasonable soil moisture time series, although a formal calibration was not completed. Layer thickness is 1 cm. The 2008 rainfall record from Marshall was used to force the model and the output was compared to the GPS and *in situ* measures of soil moisture.

VI. Results

[15] showed results from April 9, 2008 to June 30, 2008 (84 days) for a single GPS receiver with choke-ring antenna covered with a radome. The start date was chosen to avoid most of the winter days with snow. In this study we have extended the time series to November 3, 2008 (for a total of 208 days), again to avoid snow. We also compared records from an identical receiver and antenna with and without a radome. Data acquisition from the system without the radome began on May 23, 2008.

The relationship between ϕ and SMC was shown by [15] to be nearly linear for SMC values of 0.1 to 0.35 for the soil type at Marshall, with a small change in slope for SMC values $<$0.1. We have now extended the study to include the summer months of 2008, when the soil at the calibration site was very dry (Fig. 7). Although the r^2 values for the agreement between ϕ and SMC (maximum of 0.90 and minimum of 0.76) are very high, it is also clear that GPS does a very poor job of distinguishing between

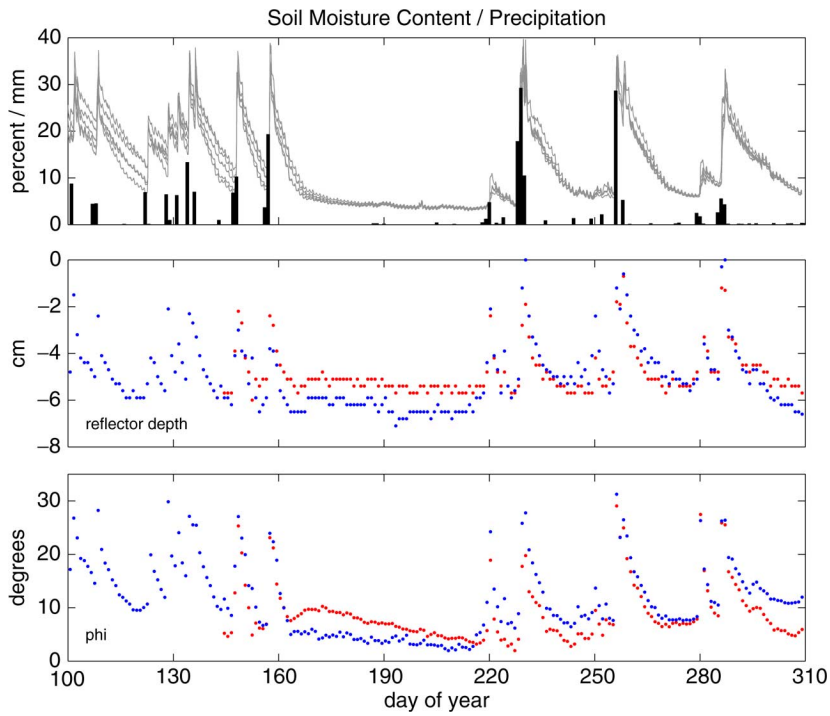

Fig. 8. Top panel: Soil moisture content (gray) for five water content reflectometers buried at a depth of 2.5 cm and daily precipitation (black); middle panel: estimated reflector depth related to the ground surface; bottom: phase offset ϕ, in degrees, with arbitrary offset removed from both time series. For both top and middle panels, red represents results for the choke-ring antenna; blue represents data from the choke-ring antenna with a radome. All data are for PRN 15.

SMC for values of 0.05–0.10. In Fig. 7, we also show the comparison between h and SMC. The reflector heights vary from a depth of 1–6 cm. In general the agreement between h and SMC is not as strong as between ϕ and SMC (r^2 0.86 to 0.68). The reflector heights, however, are more randomly distributed about the polynomial fit at SMC values <0.1 than the corresponding ϕ values. We have identified outliers for four precipitation events, and have shaded these values gray. These outliers are associated with two scenarios: 1) the first hours after precipitation events and 2) events with total precipitation amounts that are insufficient to wet the soil throughout the *in situ* measurement depth, roughly 5 cm. We expect that agreement between the different satellites will improve as we develop more sophisticated models for the SNR data.

Time series for both receivers and a single satellite are shown in Fig. 8. The GPS ϕ values closely track SMC observed by WCRs from the 2.5-cm depth. Each measured rainfall event is followed by a rise in SMC by GPS ϕ and the WCR; both decrease over a period of days to weeks. The two receivers show some variations with respect to each other which we attribute primarily to the different gain patterns for the two antenna systems. For example, for days 160–219 there was no precipitation at Marshall. Observed SMC remained nearly constant during that period, but ϕ shows a slight increase from day 160–170 for the antenna with a radome. Some of the variation in GPS measurements could be due to variations in surface roughness and vegetation. At this time we have not modeled the effects of topography or vegetation.

Although similar in some ways with our initial study, these new data provide new insights about the GPS multipath technique. In particular, we can clearly see how the GPS data respond to small and large precipitation events. The best examples of these extremes occurred on day 220 (5.9 mm of precipitation) and days 228–230 (57 mm of precipitation) respectively. The peak SMC recorded at 2.5 cm following those storms was 0.11 and 0.39, respectively. In contrast, the maximum ϕ (and minimum reflector depth) values derived from GPS are similar for each of the two precipitation events. In both cases, there was enough rainfall to move the effective GPS reflector to 2 cm below the ground surface. However, on the day 220 event, the rainfall did not fully wet the soil to a depth of 5 cm, so the probes inserted at 2.5 cm recorded only a weak response. This mismatch may yield overestimates of soil moisture following small precipitation events, when wetting fronts do not propagate to the full sensing depth of *in situ* probes.

A similar difference between GPS-derived and *in situ*-measured soil moisture exists during the early intervals of the larger precipitation events. This occurs because reflector height decreases faster than the rate at which wetting fronts propagate to the full sensing depth of the *in situ* probes, at least for the insertion depth (2.5 cm) used here. This difference is apparent during events like the day 228–230 storm (Fig. 9). During this event, the signal from the first GPS satellite (PRN 29) reflecting from the sensing area shows an earlier φ increase than SMC measured at 2.5 cm. This is consistent with our simulation of infiltration and vertical redistribution following this rainfall event. Simulated SMC in the top 1–2 cm of the profile increases rapidly after the rainfall begins, consistent with the signal from PRN 29. The rise in simulated SMC at 5 cm is lagged by several hours, consistent with the *in situ* data.

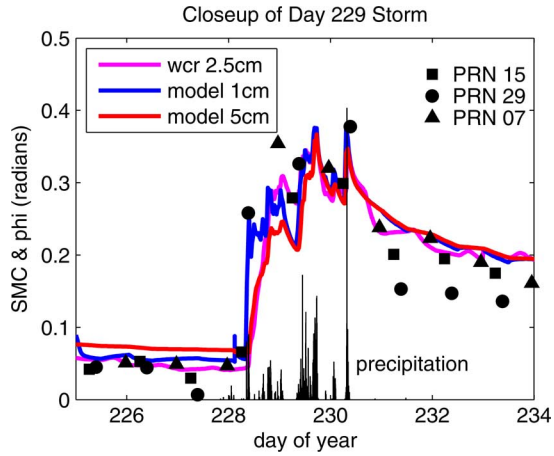

Fig. 9. Precipitation values are measured in units of 0.1 mm over 5-min intervals. GPS measurements of f are plotted in radians for southeast tracking satellites PRN 15, 29, and 7. They are arbitrarily offset to agree with TDR records on days 226–227. WCR measurements at 2.5 cm and model results for 1 and 5 cm are also shown.

VII. Future Work

Our long-term goal is to develop a retrieval algorithm to convert GPS SNR data to estimates of surface soil moisture content based on the theory developed in [16]. The soil moisture product would be available in near-real time for climate, hydrology, and ecology applications. In addition, GPS soil moisture estimates will be useful ground-truth for lower resolution (time and space) satellite estimates of soil moisture from SMOS and SMAP.

In order to achieve this goal, we must more completely understand the range of environmental factors that influence GPS SNR data. The SNR data are the product of the propagation of GPS signals through variably saturated soil and the interaction of the GPS signal with the surface topography and vegetation. The saturation state of the soil is governed by the initial saturation, the physics of flow in the vadose zone, and the local weather. We need to evaluate how different soil types and climate characteristics influence the uncertainty that exists in the SMC-ϕ and SMC-h relationships. For example, the problem of nonuniqueness in the GPS signal following small and large storms could be worse in climates characterized by numerous small storms or where soil hydraulic conductivity is low. Aside from sub-surface characteristics, variations in surface conditions must be accounted for. Because most of the Earth's terrestrial surface is covered by vegetation, we need to evaluate how vegetation amount and structure affects the SNR data. Finally, the effect of small scale variations in surface topography must be evaluated.

In addition to environmental concerns, various technological issues must be examined. For example, the amplitude of SNR oscillations is also sensitive to soil moisture [14], [16], so the best method of combining both ϕ and amplitude variations must be identified. In addition, a method must be developed to combine SNR data from numerous satellites at a single site that can minimize biases in both ϕ and h caused by differences in soil and antenna characteristics. This is critical as the number of satellites with acceptable SNR data continues to increase.

VIII. Conclusion

Estimates of signal penetration depth by geodetic-quality GPS receivers show good agreement with *in situ* soil moisture sensors buried at a depth of 2.5 cm. However, we present several points of caution related to the GPS signal penetration depth. The GPS signal will only penetrate the top centimeter or two of soil when this top centimeter is nearly saturated. As a result, immediately following the initiation of rainfall or shortly after very small rain events, the apparent soil moisture will be greater than the actual soil moisture in the top 5 cm. As a result, soil moisture determined from GPS SNR data must be used appropriately based on the depth of penetration.

With further refinement to this methodology, the existing network of GPS sensors could provide a large quantity of soil moisture data. These data will be useful for hydrological studies, weather forecasting, and climate monitoring. In addition, we anticipate that the scale of the GPS soil moisture content measurement will be extremely useful for calibrating and validating planned soil moisture satellite missions.

Acknowledgment

The authors would like to thank UNAVCO and J. Normandeau for field and archiving support, the NCAR RAL Group at Marshall for providing precipitation data, and the anonymous reviewers and editors whose comments improved this manuscript.

References

[1] P. Viterbo and A. Betts, "Impact of the ECMWF reanalysis soil water on forecasts of the July 1993 Mississippi flood," *J. Geophys. Res.*, vol. 104, no. D16, pp. 19361–19366, 1999.

[2] E. Fischer, S. Seneviratne, D. Luethi, and C. Schaer, "Contribution of land-atmosphere coupling to recent European summer heat waves," *Geophys. Res. Lett.*, vol. 34, no. 6, p. L06707, 2007.

[3] C. A. Williams and J. D. Albertson, "Soil moisture controls on canopy-scale water and carbon fluxes in an African savanna," *Water Resour. Res.*, vol. 40, p. W09302, 2004, DOI:10.1029/2004WR003208.

[4] S. Kurc and E. E. Small, "Soil moisture variations and ecosystem-scale fluxes of water and carbon in semiarid grassland and shrubland," *Water Resour. Res.*, vol. 43, no. 6, p. W06416, 2007.

[5] K. Trenberth and C. Guillemot, "Evaluation of the global atmospheric moisture budget as seen from analyses," *J. Climate*, vol. 8, no. 9, pp. 2255–2272, 1995.

[6] J. Pal and E. Eltahir, "Teleconnections of soil moisture and rainfall during the 1993 midwest summer flood," *Geophys. Res. Lett.*, vol. 29, no. 18, 2002.

[7] S. Seneviratne, D. Luethi, M. Litschi, and C. Schaer, "Land-atmosphere coupling and climate change in Europe," *Nature*, vol. 443, pp. 205–209, 2006.

[8] D. Entekhabi, E. Njoku, P. O'Neill, T. Jackson, J. Thomas, J. Entin, and I. Eastwood, "The soil moisture active/passive mission (SMAP)," presented at the IEEE Int. Geoscience Remote Sensing Symp., Boston, MA, Jul. 6–11, 2008.

[9] Y. Kerr, J. Font, P. Waldteufel, and M. Berger, "The second of ESA's opportunity missions: The soil moisture and ocean salinity mission—SMOS," *ESA Earth Observ. Quart.*, vol. 66, 2000.

[10] M. Hubert, P. Barre, B. Duesmann, and Y. Kerr, "SMOS: The mission and the system," *IEEE Trans. Geosci Remote Sens.*, vol. 46, no. 3, p. 587, Mar. 2008.

[11] M. Zreda, D. Desilets, T. P. A. Ferré, and R. L. Scott, "Measuring soil moisture content non-invasively at intermediate spatial scale using cosmic-ray neutrons," *Geophys. Res. Lett.*, vol. 35, p. L21402, 2008, 10.1029/2008GL035655.

[12] M. Martin-Neira, "A passive reflectometry and interferometry system (PARIS): Application to ocean altimetry," *ESA J.*, vol. 17, pp. 331–355, 1993.

[13] S. Katzberg, O. Torres, M. Grant, and D. Masters, "Utilizing calibrated GPS reflected signals to estimate oil reflectivity and dielectric constant: Results from SMEX02," *Remote Sens. Environ.*, vol. 100, no. 1, pp. 17–28, 2006.

[14] K. M. Larson, E. E. Small, E. D. Gutmann, A. Bilich, P. Axelrad, and J. Braun, "Using GPS multipath to measure soil moisture fluctuations: Initial results," *GPS Solutions*, vol. 12, no. 3, pp. 173–177, Jul. 2008, DOI:10.1007/s10291-007-0076-6.

[15] K. M. Larson, E. E. Small, E. D. Gutmann, A. Bilich, J. J. Braun, and V. U. Zavorotny, "Use of GPS receivers as a soil moisture network for water cycle studies," *Geophys. Res. Lett.*, vol. 35, p. L24405, 2008, DOI:10.1029/2008GL036013.

[16] V. U. Zavorotny, K. M. Larson, J. J. Braun, E. E. Small, E. D. Gutmann, and A. L. Bilich, "A physical model of GPS multipath caused by land reflections: Toward bare soil moisture retrievals," *IEEE J. Sel. Topics Appl. Earth Obs. Remote Sens.*, vol. 3, no. 1, Mar. 2010.

[17] P. Ferré, J. Knight, D. Rudolph, and R. Kachanoski, "The sample areas of conventional and alternative time domain reflectometry probes," *Water Resour. Res.*, vol. 34, pp. 2971–2979, 1998.

[18] K. Hudnut, F. Wyatt, J. Galetzka, and S. Dockter, "SCIGN radomes and adaptors," presented at the IGS Network Systems Workshop, Annapolis, MD, Nov. 2–6, 1998.

[19] P. Misra and P. Enge, *Global Positioning System: Signals, Measurements, and Performance*. Lincoln, MA: Ganga-Jamuna, 2006, p. 569.

[20] J. K. Ray and M. E. Cannon, "Synergy between global positioning system code, carrier, and signal-to-noise ratio multipath errors," *J. Guid. Contr. Dynam.*, vol. 24, pp. 54–63, 2001.

[21] K. Larson, A. Bilich, and P. Axelrad, "Improving the precision of high-rate GPS," *J. Geophys. Res.*, vol. 112, p. B05422, 2007, DOI:10.1029/2006JB004367.

[22] A. Bilich, P. Axelrad, and K. M. Larson, "Scientific utility of the signal-to-noise ratio (SNR) reported by geodetic GPS receivers," in *Proc. ION GNSS*, Ft. Worth, TX, Sep. 26–28, 2007.

[23] D. Masters, P. Axelrad, and S. Katzberg, "Initial results of land-reflected GPS bistatic radar measurements in SMEX02," *Remote Sens. Environ.*, vol. 92, no. 4, pp. 507–520, 2002, DOI:10.1016/J.RSE.2004.05.016.

[24] W. H. Press and G. B. Rybicki, "Fast algorithm for spectral analysis of unevenly spaced data," *Astrophys. J.*, vol. 338, pp. 277–280, 1989.

[25] G. C. Topp, J. Davis, and A. Annan, "Electromagnetic determination of soil water content: Measurements in coaxial transmission lines," *Water Resour. Res.*, vol. 16, pp. 574–582, 1980.

[26] E. E. Small, "Climatic controls on diffuse groundwater recharge in semiarid environments of the southwestern United States," *Water Resour. Res.*, vol. 41, p. W04012, 2005, DOI:10.1029/2004WR003193.

Kristine M. Larson received the B.A. degree in engineering sciences from Harvard University, Cambridge, MA, in 1985, and the Ph.D. degree in geophysics from the Scripps Institution of Oceanography, University of California at San Diego, La Jolla, in 1990.

She was a member of the technical staff at JPL from 1988–1990. Since 1990, she has been a professor in the Department of Aerospace Engineering Sciences, University of Colorado, Boulder. Her research interests are focused on developing new applications and techniques for GPS.

John J. Braun received the B.A. degree in physics and mathematics in 1991 from the University of Colorado, Boulder, and the PhD. degree from the Department of Aerospace Engineering Sciences, University of Colorado, in 2004.

He is a project scientist within the COSMIC program at the University Corporation for Atmospheric Research, Boulder. His research interests include developing new techniques and using GNSS observations to study the Earth and its environment, particularly the water cycle.

Eric E. Small received a B.A. degree in geological sciences from Williams College in 1993 and the Ph.D. degree in earth sciences from the University of California at Santa Cruz in 1993.

He is an Associate Professor in the Department of Geological Sciences, University of Colorado, Boulder. His research is focused on land surface hydrology.

Valery U. Zavorotny (M'01–SM'03) received the M.Sc. degree in radio physics from Gorky State University, Gorky, Russia, in 1971, and the Ph.D. degree in physics and mathematics from the Institute of Atmospheric Physics, USSR Academy of Sciences, Moscow, in 1979.

From 1971 to 1990, he was a Research Scientist with the Institute of Atmospheric Physics of the USSR Academy of Sciences, Moscow. In 1990, he joined Lebedev Physical Institute, Moscow, Russia. In 1991–2000, he was a CIRES Research Associate in the Environmental Technology Laboratory of the National Oceanic and Atmospheric Administration (NOAA), Boulder, CO, and became a NOAA/ETL physicist in 2000. His research interests include theory of wave propagation through random media, wave scattering from rough surfaces, and ocean and land remote sensing applications.

Dr. Zavorotny is a member of URSI (Commission F) and the American Geophysical Union.

Ethan D. Gutmann received the B.A. degree in geology and computer science from Williams College in 1999 and the Ph.D. degree in geological sciences from the University of Colorado, Boulder, in 2008.

He is a postdoctoral fellow at the Research Applications Laboratory, National Center for Atmospheric Research, Boulder.

Andria L. Bilich received the B.S. degree in geophysics from the University of Texas, Austin, in 1999, and the Ph.D. degree in aerospace engineering sciences from the University of Colorado, Boulder, in 2006.

She is a Geodesist with the National Geodetic Survey's Geosciences Research Division. Her research interests include GPS multipath characterization, GNSS antenna calibration, and precision improvements to GNSS positioning for geoscience applications.